

G4-Attention: Deep Learning Model with Attention for predicting DNA G-Quadruplexes

Shrimon Mukherjee,[†] Pulakesh Pramanik,[‡] Partha Basuchowdhuri,^{*,†} and Santanu
Bhattacharya^{*,‡,¶,§,||}

[†]*School of Mathematical & Computational Sciences, Indian Association for the Cultivation
of Science, Kolkata, India*

[‡]*School of Applied & Interdisciplinary Sciences, Indian Association for the Cultivation of
Science, Kolkata, India*

[¶]*Technical Research Center, Indian Association for the Cultivation of Science, Kolkata,
India*

[§]*Department of Organic Chemistry, Indian Institute of Science, Bangalore, India*

^{||}*Department of Chemistry, Indian Institute of Science Education and Research Tirupati,
Andhra Pradesh, India*

E-mail: partha.basuchowdhuri@iacs.res.in; sb23in@yahoo.com,sb@iisc.ac.in

Abstract

G-Quadruplexes are the four-stranded non-canonical nucleic acid secondary structures, formed by the stacking arrangement of the guanine tetramers. They are involved in a wide range of biological roles because of their exceptionally unique and distinct structural characteristics. After the completion of the human genome sequencing project, a lot of bioinformatic algorithms were introduced to predict the active G4s regions *in vitro* based on the canonical G4 sequence elements, G-richness, and

G-skewness, as well as the non-canonical sequence features. Recently, sequencing techniques like G4-seq and G4-ChIP-seq were developed to map the G4s *in vitro*, and *in vivo* respectively at a few hundred base resolution. Subsequently, several machine learning approaches were developed for predicting the G4 regions using the existing databases. However, their prediction models were simplistic, and the prediction accuracy was notably poor. In response, here, we propose a novel convolutional neural network with Bi-LSTM and attention layers, named G4-attention, to predict the G4 forming sequences with improved accuracy. G4-attention achieves high accuracy and attains state-of-the-art results in the G4 prediction task. Our model also predicts the G4 regions accurately in the highly class-imbalanced datasets. In addition, the developed model trained on the human genome dataset can be applied to any non-human genome DNA sequences to predict the G4 formation propensities.

Introduction

Guanine-rich DNA and RNA sequences have the ability to fold into four-stranded non-canonical secondary structures known as G-quadruplexes (G4s).¹ These functional secondary structures were discovered in the late 80's² and have displayed important cellular roles in living cells.³ G4s are structurally a self-stacked arrangement of the G-quartets, a square planar organized structure formed by four guanine nucleotides connected through Hoogsteen-type of hydrogen bonding, one on top of another via π - π stacking interaction (Fig. 1).^{4,5} These structures can form kinetically, but may be stabilized thermodynamically in the presence of monovalent cations such as Na^+ , and K^+ under physiological conditions.^{6,7} Even though G4s are spontaneously formed from four consecutive tracts of three or more guanines separated by loops having various lengths under *in vitro* conditions, many non-canonical G4s, that is G4s with longer loops, mismatches, and bulges, have been recently reported. It indicates that sequence patterns are less strict characteristics for the formation of G4s than previously believed.^{8,9} Depending upon the physiological conditions, syn- or anti-conformation of the

glycosidic bond, and intrinsic features of the sequence, G4s can adopt various topologies such as parallel, anti-parallel, and hybrid G4s.¹⁰ In addition, G4s can be formed from one (unimolecular), two (bimolecular), or four (tetramolecular) distinct strands with different topologies.^{11,12} Furthermore, the structural integrity is affected by the number of consecutive G-quartets, loop length, and the composition of nucleotides in loop regions.^{13,14}

The G4 motifs were significantly distributed in the telomeric regions of chromosomes, gene promoter regions, DNA replication origins, 5'-untranslated region (UTR), first intron, and exon regions of various genes.¹⁵⁻¹⁹ Recently, G4s were visualized using an immunofluorescence assay, which demonstrates their existence in cells and tissues.²⁰⁻²² Several investigations have further revealed their potential involvement in critical biological functions such as telomeric stability, DNA replication, gene transcription, mRNA translation, and DNA repair.²³⁻²⁸ For example, in 85-90% of cancer cells, up-regulation of telomerase enzyme was observed which blocks the activation of cell apoptosis machinery by restoring the telomeric length during the cell division process.^{29,30} The terminal 3'- telomeric DNA can down-regulate the telomerase activity by forming G4s; thereby uncontrolled tumor cell proliferation is inhibited by the activation of apoptosis machinery.²⁹ Furthermore, G4s can repress the expression of various oncogenes such as MYC, KIT, Bcl-2, KRAS, HRAS, and VEGF found in cancer cells.³¹⁻³⁶ G4s are therefore believed to be associated with human diseases like cancer, neurological disorders, and ageing and have emerged as a potential target for therapeutic intervention.^{27,37-39}

Because of the significant regulatory roles of G4s in cellular processes, numerous mathematical and computational algorithms were developed to predict the location of active putative quadruplex sequence (PQS) throughout the human genome with high accuracy.⁴⁰ The first PQS detection tool, quadparser was developed using the classical regular expression matching technique in C++ and Python scripting language.⁴¹ This tool was used to detect all matching occurrences of canonical G4 motifs across the human genome by using a strict sequence pattern $G_{3-5}N_{1-7}G_{3-5}N_{1-7}G_{3-5}N_{1-7}G_{3-5}$; where G and N represent guanine, and

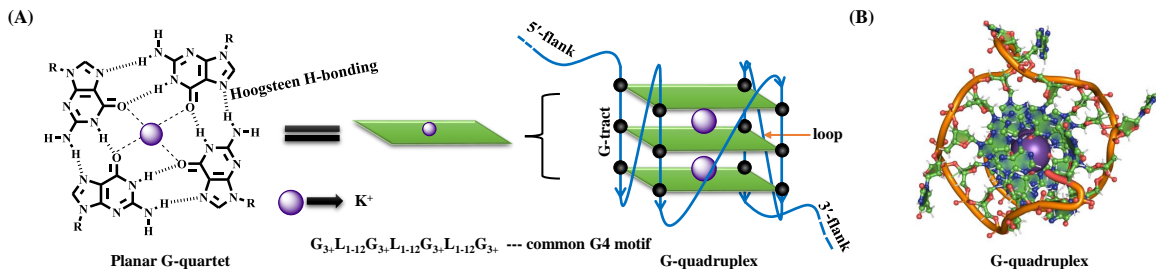


Figure 1: Schematic representation of canonical G-quadruplex structures in DNA. (A) Structure of planar G-quartet formed by four guanine bases through Hoogsteen type of H-bonding, and a central cation usually K^+ . The G-quadruplex structures are commonly comprised of three stacks planar G-quartet top to one another via $\pi - \pi$ stacking interaction. (B) Top-view of human promoter G4 found in *c-MYC* gene (PDB : 1XAV).

any other nucleotide respectively. This model identified around 376,000 unimolecular PQS motifs in the human genome (*hg19* reference). One of the main flaws of this tool is that it provides a yes/no binary output without considering the structural stability and *in-vivo* folding propensity. Since 2005, methods that were developed on the PQS motifs, which fit the regular expression mentioned above, have been used in the majority of the research studies to predict the G4 propensity.⁴²⁻⁴⁴ More recently, a similar kind of regular expression matching tool, AllQuads has been developed to identify the inter-molecular G4s.⁴⁵ Meanwhile, several *in-vitro* and *in-vivo* experiments proved the existence of non-canonical i.e., imperfect G4s along with canonical G4s in the human genome.⁴⁶ Afterward, new methods were developed to identify imperfect G4s by incorporating the features of the newly-found imperfect G4 and by updating the algorithms incrementally. For instance, ImGQfinder⁴⁷ can detect the non-canonical intra-molecular PQS motif with a single bulge or mismatch, and pqsfinder^{48,49} recognizes G4s folded from G-runs with flaws such as bulges, mismatches, and G4s with longer loops. In addition, pqsfinder^{48,49} also gives each hit an integer score, which represents the predicted stability of the folded G4s. Further, an algorithm based on a sliding window approach, G4Hunter⁵⁰⁻⁵² was developed to compute the quadruplex propensity score based on *G-richness* and *G-skewness* of a given sequence. Overall, these tools contributed significantly to the G4 exploration. However, due to the lack of vast biophysi-

cal and biochemical databases, these tools cannot perfectly predict the G4s sequences and stability.

Recently, G4-seq⁵³ and G4-ChIP-seq⁵⁴ types of experimental methods were implemented to map G4s *in vitro* and *in vivo* respectively. Following that, new machine and deep learning types of artificial intelligence approaches were used to predict the G4s much more accurately using the sequencing databases. For example, Quadron,⁵⁵ a machine learning algorithm, was trained using a large database of experimental G4 regions, obtained by the G4-seq techniques in the human genome. This algorithm can detect the G4 sequences and assign a score of the detected G4s, which represents their formation propensity *in vitro*. Other deep learning models, such as PENGUINN,⁵⁶ and G4Detector,⁵⁷ a convolutional neural network (CNN) were also developed to predict the G4 regions *in vitro*. Since all of these models were constructed throughout the training process with the G4-seq database, new models were then going to be developed for predicting G4 sequences in cells using G4-ChIP-seq peak DNA sequences. For instance, DeepG4⁵⁸ used a CNN to predict cell-type specific active G4 regions, which is trained using a combination of G4-seq, and G4 ChIP-seq DNA sequences with chromatin accessibility measures (ATAC-seq). Further, epiG4NN⁵⁹ was developed which uses a ResNet⁶⁰ based architecture for G4s prediction in cells. Despite the advancement of numerous machine and deep learning models using the existing databases, the prediction accuracy was quite poor and requires further improvement. In addition, all the prediction models were very simplistic. The prediction accuracy can be enhanced by incorporating additional layers, such as GRU, LSTM, attention, and dilated convolution layers,⁶¹ into the networks. Developing more sophisticated models is imperative for achieving improved prediction accuracy.

In this study, we proposed a novel architecture named G4-Attention to predict the G4-forming sequences with improved prediction accuracy. Our work makes the following contributions:

- To the best of our knowledge, we are the first ones to introduce Bi-LSTM and attention

layers on top of CNN to predict the G4-forming sequences. The experimental results showed that our model achieves state-of-the-art results in the G4 sequences prediction task.

- To investigate the robustness of our model, we apply it to highly class-imbalanced scenarios.
- In addition, we validate G4-Attention trained on human-genome dataset on non-human genome dataset.

Materials and Methods

Datasets

In this section, we will discuss about the datasets used to train and evaluate our proposed model G4-Attention.

G4-seq_{IB}. We acquired human genome named *hg19*/GRCh37 from the the UCSC Genome Browser¹. We employed the *Python re* package to extract PQS sequences, expanding the conventional definitions of G4. This was achieved using specific regular expression patterns: $[G^{3+}L^{1-12}]^{3+}G^{3+}$, a standard G4 pattern with elongated loop length;⁶² $[GN^{0-1}GN^{0-1}GL^{1-3}]^{3+}GN^{0-1}GN^{0-1}G$, a enlarged G4 pattern with probable G-run breaks;⁶³ and $[G^{1-2}N^{1-2}]^{7+}G^{1-2}$, an uneven G4 pattern,⁶⁴ where $L \in \{A, T, C, G\}$ and $N \in \{A, T, C\}$. We filtered the redundant and nested G4 sequences by taking into consideration at least one nucleotide. Additionally, we calculated the total number of guanines, ensuring that they are greater than or equal to 12, to facilitate the formation of three-layered G4s. This search was conducted on both strands. For each PQS, the corresponding G4 score was determined by analyzing the experimental peaks and calculating the mean of the con-

¹<http://genome.ucsc.edu/>

tinuous signal in the *.bedgraph* format. In the instances where the PQS coordinate lacked an associated signal, the score was set as 0.0. For training purposes, G4 labels were obtained from the G4P ChIP-seq study performed on A549 cell lines, as present in the GEO database with accession number GSE133379. The top 5% of normalized experimental scores were classified as the “positive” class and the remaining are classified as the “negative” class². In this dataset most of the PQS had zero scores, therefore, the classes are highly imbalanced. Thus, we applied our model in a highly imbalanced scenario, which helps us establish the robustness of our model. The distribution of positive and negative classes is shown in Table 1. The dataset was divided into two subparts: train and test, where the test subpart includes all the PQS belonging to chromosomes 1, 3, 5, 7, 9 and the train subpart includes all the PQS belonging to chromosomes 2, 4, 6, 8, 10-22, X, Y. The number of training and testing samples present in the dataset are 1,494,884 and 610,953.

Table 1: Distribution of Positive and Negative Samples in the G4-seq_{IB} Dataset

Sample Type	Percentage	Number of Samples
Positive	5.0%	105,286
Negative	95.0%	2,000,551

Table 2: Dataset Statistics for G4-seq_B dataset

	K^+		$K^+ + \mathbf{PDS}$	
	# Training	# Testing	# Training	# Testing
Random	768,256	70,736	2,427,160	231,026
Dishuffle	794,186	74,330	2,510,078	242,730
PQ	784,576	75,457	1,360,065	131,206

G4-seq_B. In the present study, we further extend the application of our model G4-Attention to a balanced dataset, initially introduced in this work.⁵⁷ This dataset covers whole-genome G4 measurements across four species⁵⁷ (human, mouse, zebrafish, and drosophila)³. Here,

²As mentioned in this work⁵⁹

³Mouse, zebrafish and drosophila are used in the case study.

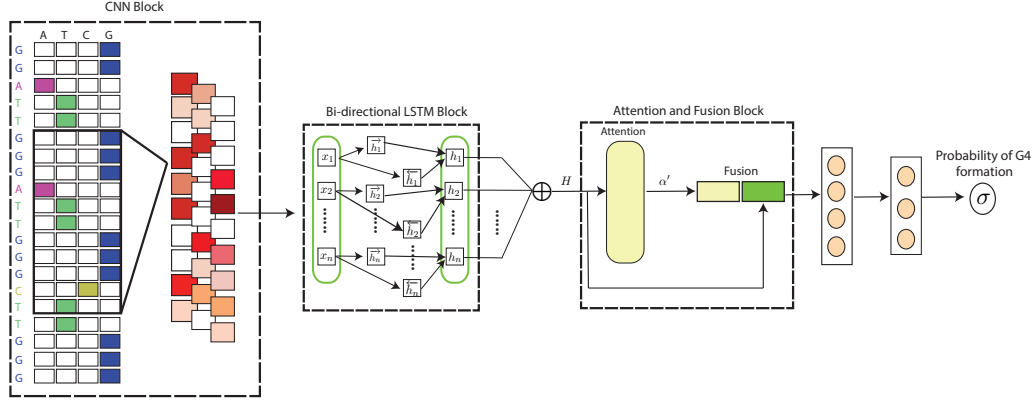


Figure 2: Schematic diagram of our proposed model **G4-Attention**. Our Proposed model has three blocks: CNN block, Bi-LSTM block and finally Attention Fusion block.

we focus exclusively on the whole-genome data about humans for training and evaluation of our model. As mentioned in this work,⁵⁷ we obtained two FASTA files for the K^+ and K^+ + PDS for the human genome, respectively and we mentioned these sets as the positive sets in G4 prediction problem. To generate the negative examples for each positive example, we followed the technique used by Barshai et. al.⁵⁷ and we constructed three datasets.

- Random: for every positive sequence, we obtained an equivalent sequence, matching in length, from a randomly selected coordinate within the human genome.
- Dishuffle: for every positive sequence, we randomized its nucleotide arrangement while maintaining the frequencies of dinucleotides.⁶⁵
- PQ: predicted G4s in the genome using the regular expression $[G^{3+}N^{1-12}]G^{3+}$, where N represents any nucleotide.

For all three sets of data, we consider the genome sequences belonging to Chromosome 1 as the test sets and the remaining sequences as the training sets. The overall dataset statistics are depicted in Table 2.

G4-Attention Neural Network Architecture

This section starts by outlining the general idea of our proposed neural network framework namely G4 quadruplex prediction by utilizing Attention mechanism (**G4-Attention**)⁴ for predicting whether a genome sequence forms G4 or not, followed by a detailed discussion about the different components of our proposed framework. The overview of our proposed architecture is depicted in Figure 2.

Encoding of the Genome Sequence

The nucleotide in each position of a genome sequence is represented by a 4-dimensional one-hot vector for training and testing as $A = (1, 0, 0, 0)$, $T = (0, 1, 0, 0)$, $C = (0, 0, 1, 0)$ and $N = (0, 0, 0, 0)$. We denote the one-hot vector representation for a sequence as $\mathbf{S}^{\mathbf{O}}$ of shape $L \times 4$, where L is the sequence length. $\mathbf{S}^{\mathbf{O}}$ carries the raw information of the sequence.

Feature extraction using CNN

We automatically extract local features of $\mathbf{S}^{\mathbf{O}}$ using a Conv1D layer. Conv1D layer is a popular architecture in genomics that automatically learns important features from raw sequences.⁶⁶ More specifically, the Conv1D layer utilizes $\mathbf{S}^{\mathbf{O}}$ as the input raw information of the sequence of shape $n \times 4$ and applies a kernel (Θ_c) of shape $K \times F$ where K is the kernel size and F is the number of kernels. The output of the CNN is x_f , $x_f = \sigma(x_f^i)$, $x_f^i \in \mathcal{R}^{n \times F}$, where σ is a non-linear function, applied on the intermediate value x_f^i obtained through Conv1D.

Feature extraction using Bi-directional LSTM

We pass the learned feature representation of $\mathbf{S}^{\mathbf{O}}$ using our Conv1D block, which is x_f to a Bi-LSTM layer, which captures the dependencies between the characters in a sequence of length n . We get the output representation $H \in \mathcal{R}^{2d_l}$, where d_l represents the number of

⁴Our source code will be available upon acceptance of this work

output units used in each LSTM cell. We use Eq. 1 for the execution of the LSTM.

$$\begin{aligned}
 \vec{h}_t &= \overrightarrow{LSTM}(x_f, h_{n-1}) \\
 \overleftarrow{h}_t &= \overleftarrow{LSTM}(x_f, h_{n+1}) \\
 H &= (\vec{h}_n \cdot \overleftarrow{h}_n)
 \end{aligned}
 \tag{1}$$

Attention and Fusion block of G4-Attention

Here, we use a simplified form of attention mechanism popularly used in natural language processing.⁶⁷ The attention block calculates α for H and the values of α quantify the importance of each nucleotide in a genome sequence. We calculate α using the Eq. 2.

$$\alpha = H\theta_A + b_A
 \tag{2}$$

where θ_A is the trainable weight in the attention module, b_A is the bias. α is fed into the softmax layer and is normalized to α' using the following Eq. 3.

$$\alpha' = \frac{e^\alpha}{\sum_j e^{\alpha_j}}
 \tag{3}$$

The fusion block receives H and α' from the Bi-LSTM and the attention blocks and subsequently computes the final feature tensor X using the Eq. 4.

$$X = \alpha'H
 \tag{4}$$

Prediction Layer

X is fed into two fully connected neural networks and finally, we applied a sigmoid activation function as the task is a binary classification problem. We used the binary cross-entropy loss

using the Eq. 5 to train the **G4-Attention** model.

$$L = -\frac{1}{B} \sum_{i=1}^B [Y_i \cdot \log(Y_i) + (1 - Y_i) \cdot \log(1 - Y_i)] \quad (5)$$

where $Y_i = \text{sigmoid}(X_i)$ and B is the number of data samples in one batch. Again, in G4-seq_{IB}, the number of positive samples is suppressed by the number of negative samples by a large margin, resulting in the network potentially being biased towards the negative samples and failing to correctly identify positive samples when Eq. 5 is considered as the loss function. This issue is tackled by implementing balanced class weights $W_P = \frac{|D|}{|C| \cdot \text{freq}_P}$ and $W_C = \frac{|D|}{|C| \cdot \text{freq}_N}$ for positive and negative samples respectively. Here $|D|$ is the number of samples present in the dataset and $|C|$ is the total number of classes. We slightly modify Eq. 5 to introduce class weights in binary classification loss as shown in Eq. 6.

$$L = -\frac{1}{B} \sum_{i=1}^B [W_P \cdot Y_i \cdot \log(Y_i) + W_N \cdot (1 - Y_i) \cdot \log(1 - Y_i)] \quad (6)$$

Parameter Settings

In this work, we fixed the length of the genome sequence to 124^{57} for G4-seq_B dataset, and for G4-seq_{IB} we fixed the length of the genome sequence to 1000.⁵⁹ Here, we considered one 1DCNN and one Bi-LSTM layer to train our framework G4-Attention. We trained it for 10 epochs using Adam⁶⁸ for optimization with a learning rate of 0.001. We utilized a batch size of 1024 with a seed value of 123 to train our model. We used PyTorch-Ignite⁵ framework for our implementation. One NVIDIA A6000 48GB GPU, and one NVIDIA A100 80GB GPU were used to train and evaluate our model G4-Attention.

⁵<https://pytorch.org/ignite/index.html>

Results

Evaluation Criteria

We determine the performance of our proposed model using two widely used metrics; the area under the ROC curve (AUC) and the area under P-R curve (AUPRC) using the Eqns. 7 and 8 respectively.

$$TPR = \frac{TP}{(TP + FN)} \quad FPR = \frac{FP}{(FP + TN)} \quad (7)$$

$$Prec = \frac{TP}{(TP + FP)} \quad Rec = \frac{TP}{(TP + FN)} \quad (8)$$

where TP , FP and FN are true-positive, false-positive and false-negative respectively. The AUC measures the performance of the model by calculating the relationship between the false-positive rate (FPR) and the true-positive rate (TPR) at different probabilities or thresholds. However, AUC is not optimal for imbalanced classification problems;⁵⁹ therefore we additionally evaluate AUPRC to determine precision and recall of positive G4 samples in class imbalanced scenarios.

Research Questions

In this section, we pose a few research questions which are central to our research work.

- **RQ1.** To what extent does our model accurately predict the G4 propensities of a given genome sequence?
- **RQ2.** What is the effectiveness of our model in scenarios characterized by class imbalance, specifically in situations where the quantity of positive samples is substantially lower than that of negative samples?
- **RQ3.** How does our model perform in cross-domain testing, specifically in predicting G4 formation in non-human species?

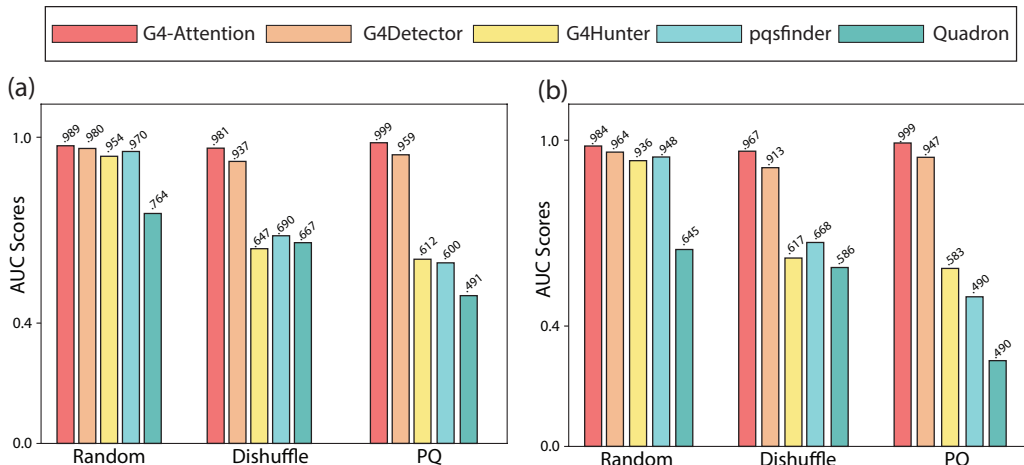


Figure 3: G4-Attention outperforms all the existing techniques across all negative types (a) K^+ and (b) $K^+ + PDS$ on held out chromosome 1 on G4-seq_B dataset.

Model Comparison in Balanced Scenerio

In relation to RQ-1, we compare our model with the existing computational methods that are used to predict G4 sequences in the balanced dataset G4-seq_B. Here, we make a comparison between our model and 4 state-of-the-art methods, including Quadron,⁵⁵ pqsfinder,^{48,49} G4hunter^{50–52} and G4Detector.⁵⁷ All methods are applied in identical experimental conditions and utilize the optimal parameters as specified in their respective research articles.

G4hunter: utilizes domain knowledge-based rules, using a sliding window approach to determine G4 propensity by analyzing the GC content in a specific sequence.

pqsfinder: This method identifies G4s by locating G-tracts in the genome sequence.

Quadron: In this approach, the objective is to predict the robustness of the DNA G4 structure utilizing machine learning.

G4Detector: In this approach, the CNN-based architecture incorporates both raw sequence data and RNA secondary structure information as input.

Fig. 3 (a) and (b) exhibit that our proposed architecture produces current state-of-the-art results on three negative types on two stabilizers K^+ and $K^+ + PDS$. The network trained solely on sequence information exhibited notable performance on the K^+ dataset, achieving

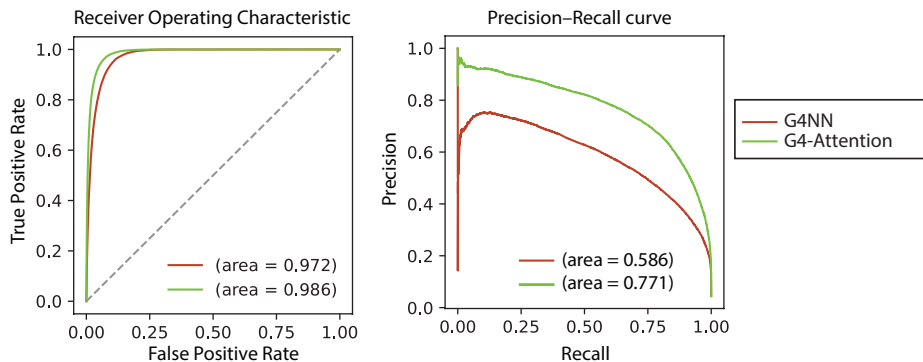


Figure 4: The performance of G4-Attention on test chromosomes 1, 3, 5, 7, 9 in the G4-seq_{IB} dataset is depicted in this figure, where both AUROC and AUPRC are present.

AUC scores of 0.989, 0.981, and 0.999 for random, dishuffle, and PQ negatives, respectively. This performance was benchmarked against established baselines, including G4Detector, G4Hunter, pqsfinder, and Quadron. This performance was in comparison to the G4Detector method, which incorporates RNA structure probabilities into the input feature. In this study, we trained and tested G4-Attention against the PQ negative set, which achieved the highest AUC score of 0.999, indicating superior performance in the most challenging of the three proposed classification problems.⁵⁷ The negative set of PQ is formulated from genomic regions characterized by a G-rich regular expression, thereby demonstrating the capability of our method to predict G4 formation in genomic segments populated with G-rich sequences.⁵⁷ In the analysis of the dataset involving K^+ + PDS stabilizers, G4-Attention achieved remarkable AUC scores, registering 0.984, 0.967, and 0.999 for random, dishuffle, and PQ evaluations, respectively, which achieves current state-of-the-art on K^+ + PDS dataset.

Model Comparison in Imbalanced Scenario

In this section, we turned our attention to RQ-2 to understand whether our proposed method G4-Attention performs accurately in practical situations i.e., for the negatively skewed dataset. The occurrence of G4 structures within the human genome exhibits a pronounced negative skewness. The G4-seq experiment revealed approximately 1,400,000 G4s distributed throughout the human genome.⁶⁹ Given the human genome’s composition of over six billion

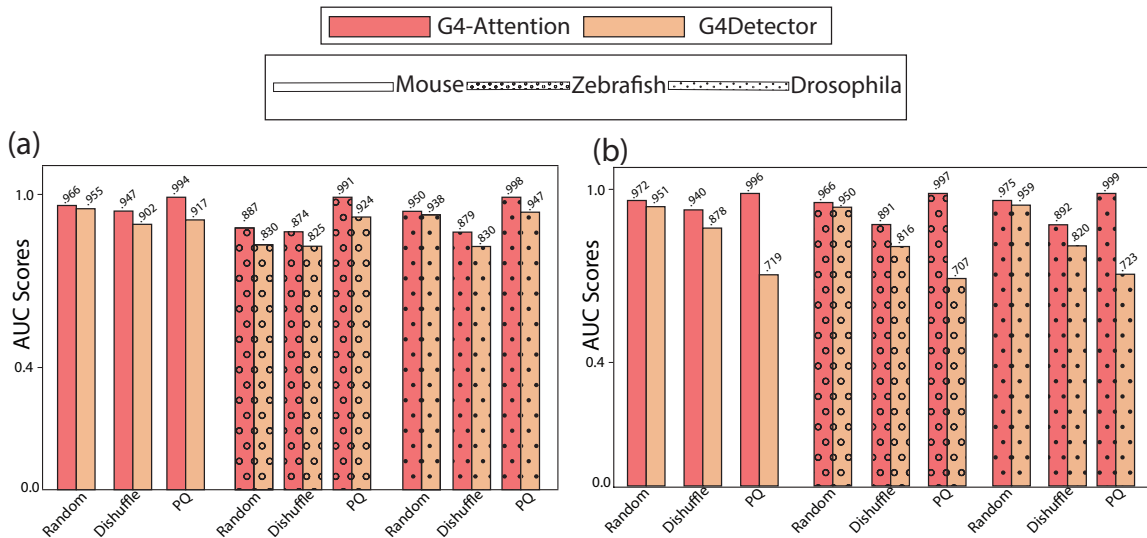


Figure 5: The comparative analysis of G4-Attention’s performance on novel datasets from three distinct species against G4Detector is illustrated in the figure. This evaluation specifically focuses on the AUC scores on (a) K^+ datasets and (b) K^+ + PDS datasets, including data from mouse, zebrafish, and drosophila species. AUC scores for G4-Attention and G4Detector are indicated at the top of the bars.

nucleotides, the frequency of G4 can be estimated to occur approximately every 4,200 to 15,000 nucleotides. This drives the necessity to assess the efficacy of G4-Attention when applied to a dataset with a negative skewness. Due to the class imbalance, we measured the performance of G4-Attention using the AUPRC, in addition to AUC.

We use the class imbalanced dataset named G4-seq_{IB} and measure the performance of G4-Attention against the baseline model G4NN,⁵⁹ a ResNet⁶⁰ based architecture. From Table 1 we observe that the dataset G4-seq_{IB} consists of high negative skewness. To address this problem we used Eq. 6 as the loss function to optimize the model parameters of the G4-Attention. From Fig. 4 we observe that it produces AUC and AUPRC scores of 0.986 and 0.771 respectively, which outperforms the existing model G4NN⁵⁹ by a large margin. This finding establishes that our model works equally well in negatively skewed datasets, thereby proving the robustness of our model.

Performance of G4-Attention in Non-Human Species

To address RQ-3, we applied our model G4-Attention on the multiple species dataset reported by Barshai et. al.,⁵⁷ which provides a perfect test set for G4-Attention. Here, we measured the ability of our model G4-Attention in a cross-domain testing scenario. We utilized G4-Attention, trained on the human genome, to conduct zero-shot testing on a range of non-human species, none of which were included in the initial training dataset. From Fig. 3, it is observed that G4-Attention produces good results in the leave-chromosome-out test data. However, this might indicate potential overfitting of G4-Attention to the G4-seq_B dataset, or it may reveal biases specific to the human genome or human cells.

Fig 5 (a) and (b) show that G4-Attention produces excellent predicting performance for non-human species mouse, zebrafish, and drosophila on two stabilizers K^+ and K^+ + PDS. G4-Attention predictions achieve AUC scores of 0.966, 0.947, and 0.994 on three negative datasets random, dishuffle, and PQ respectively on K^+ stabilizers. These results outperform existing baseline G4Detector results by large margins. Again, on K^+ + PDS dataset, our model produces AUC scores of 0.972, 0.940, and 0.996 on random, dishuffle, and PQ negatives respectively, outperforming the results of G4Detector. For zebrafish, our model produces AUC scores of 0.887, 0.874, and 0.991 for random, dishuffle, and PQ respectively for K^+ stabilizers, outperforming the AUC scores produced by G4Detector. Similar results are shown on K^+ + PDS for zebrafish. Finally, for drosophila, G4-Attention produces AUC scores of 0.950, 0.879, and 0.998 on random, dishuffle, and PQ negatives on K^+ dataset, which surpass the results of the G4Detector. Similar results are shown on K^+ + PDS for drosophila. These findings indicate that our model G4-Attention, despite being trained on the human genome, does not exhibit bias towards it. Consequently, G4-Attention can be applied to the genomes of various species to accurately predict G4 formation.

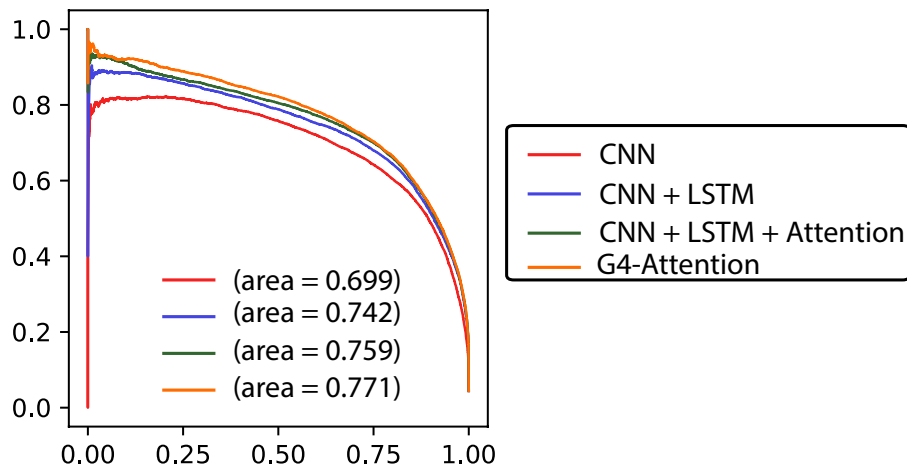


Figure 6: A series of ablation studies were performed on the class imbalance dataset G4-seq_{IB}. The precision-recall curves (AUPRC) have been shown.

Ablation Study

Here, we perform a series of ablation experiments on class imbalanced dataset G4-seq_{IB} for our proposed model G4-Attention. Initially, we consider CNN as our baseline model. Here, we take 1D CNN to extract features from the genome sequence and then we predict whether the genome sequence has G4 propensities or not. It achieves an AUPRC score of 0.699. Subsequently, we introduce an LSTM layer on top of the CNN layer and this model produces an AUPRC score of 0.742. Furthermore, we introduce an attention layer on the CNN + LSTM model, which increases the model performance as it produces an AUPRC score of 0.759. Finally, we implement our model G4-Attention by replacing the LSTM layer in the CNN + LSTM + Attention model with a Bi-LSTM layer and this architecture produces an AUPRC score of 0.771. Fig. 6 shows that G4-Attention contributes significantly towards achieving state-of-the-art results on this task. Here, we take G4-seq_{IB} for conducting ablation experiments because the prediction of positive G4s on the datasets with high negative skewness is a challenging task. Since the dataset is class imbalanced, we take the AUPRC metric to conduct the ablation experiments.

Conclusion

In this work, we present a novel framework G4-Attention for the task of predicting G4 formation in a genome sequence. Our model uses CNN, Bi-LSTM, and an attention-based network to predict the G4 formation of a genome sequence. We carried out our experiments on two datasets. One is a balanced dataset and another is a class imbalanced dataset with high negative skewness. Experimental results show that our model produces new state-of-the-art results on these datasets. We also carried out experiments on the genome sequences of non-human species such as mouse, zebrafish, and drosophila. Experimental results show that our model trained on the human genome not only produces excellent results on in-domain test data but also produces state-of-the-art results for out-domain test data as well. This shows that we can apply G4-Attention on any genome sequence to predict its G4 propensity. These observations, collectively, lead to the overall conclusion that we have successfully developed a deep-learning model with Bi-LSTM and attention layers using human genome sequences, named G4-Attention which predicts G4 DNA formation across diverse datasets, including both balanced and class-imbalanced sets, spanning various species such as human, mouse, zebrafish, drosophila, in comparison to alternatives models.

Competing interests

The authors declare that there are no conflicts of interest.

Author contributions statement

Prof. SB and Prof. PBC conceptualized the study. SM performed experimental work. SM and PP contributed to the analysis of the results and prepared the figures. SM and PP wrote the initial draft of the manuscript. SM, PP, Prof. PBC, and Prof. SB edited the manuscript.

Acknowledgement

This study was funded by the Indian Association for the Cultivation of Science (IACS), Kolkata, India. SM thanks IACS for a research fellowship. PP thanks the Council of Scientific and Industrial Research, India for a research fellowship.

References

- (1) Burge, S.; Parkinson, G. N.; Hazel, P.; Todd, A. K.; Neidle, S. Quadruplex DNA: sequence, topology and structure. *Nucleic Acids Research* **2006**, *34*, 5402–5415.
- (2) Henderson, E.; Hardin, C. C.; Walk, S. K.; Tinoco Jr, I.; Blackburn, E. H. Telomeric DNA oligonucleotides form novel intramolecular structures containing guanine·guanine base pairs. *Cell* **1987**, *51*, 899–908.
- (3) Varshney, D.; Spiegel, J.; Zyner, K.; Tannahill, D.; Balasubramanian, S. The regulation and functions of DNA and RNA G-quadruplexes. *Nature reviews Molecular Cell Biology* **2020**, *21*, 459–474.
- (4) Chaudhuri, R.; Bhattacharya, S.; Dash, J.; Bhattacharya, S. Recent update on targeting c-MYC G-quadruplexes by small molecules for anticancer therapeutics. *Journal of Medicinal Chemistry* **2020**, *64*, 42–70.
- (5) Roy, S.; Bhattacharya, S. Chemical information and computational modeling of targeting hybrid nucleic acid structures of PIM1 sequences by synthetic Pyrrole-Imidazole Carboxamide drugs. *Journal of Chemical Information and Modeling* **2022**, *62*, 6411–6422.
- (6) Jana, J.; Weisz, K. Thermodynamic Stability of G-Quadruplexes: Impact of Sequence and Environment. *ChemBioChem* **2021**, *22*, 2848–2856.

- (7) Tucker, B. A.; Hudson, J. S.; Ding, L.; Lewis, E.; Sheardy, R. D.; Kharlampieva, E.; Graves, D. Stability of the Na⁺ form of the human telomeric G-quadruplex: role of adenines in stabilizing G-quadruplex structure. *ACS Omega* **2018**, *3*, 844–855.
- (8) Jana, J.; Mohr, S.; Vianney, Y. M.; Weisz, K. Structural motifs and intramolecular interactions in non-canonical G-quadruplexes. *RSC Chemical Biology* **2021**, *2*, 338–353.
- (9) Hennecker, C.; Yamout, L.; Zhang, C.; Zhao, C.; Hiraki, D.; Moitessier, N.; Mittermaier, A. Structural polymorphism of guanine quadruplex-containing regions in human promoters. *International Journal of Molecular Sciences* **2022**, *23*, 16020.
- (10) Ma, Y.; Iida, K.; Nagasawa, K. Topologies of G-quadruplex: Biological functions and regulation by ligands. *Biochemical and Biophysical Research Communications* **2020**, *531*, 3–17.
- (11) Meier, M.; Moya-Torres, A.; Krahn, N. J.; McDougall, M. D.; Orriss, G. L.; McRae, E. K. S.; Booy, E. P.; McEleney, K.; Patel, T. R.; McKenna, S. A.; others Structure and hydrodynamics of a DNA G-quadruplex with a cytosine bulge. *Nucleic Acids Research* **2018**, *46*, 5319–5331.
- (12) Tran, P. L. T.; De Cian, A.; Gros, J.; Moriyama, R.; Mergny, J.-L. Tetramolecular quadruplex stability and assembly. *Quadruplex Nucleic Acids* **2013**, 243–273.
- (13) Hao, F.; Ma, Y.; Guan, Y. Effects of central loop length and metal ions on the thermal stability of G-quadruplexes. *Molecules* **2019**, *24*, 1863.
- (14) Bochman, M. L.; Paeschke, K.; Zakian, V. A. DNA secondary structures: stability and function of G-quadruplex structures. *Nature Reviews Genetics* **2012**, *13*, 770–780.
- (15) Phan, A. T.; Mergny, J.-L. Human telomeric DNA: G-quadruplex, i-motif and Watson–Crick double helix. *Nucleic Acids Research* **2002**, *30*, 4618–4625.

- (16) Lago, S.; Nadai, M.; Cernilogar, F. M.; Kazerani, M.; Domíniguez Moreno, H.; Schotta, G.; Richter, S. N. Promoter G-quadruplexes and transcription factors cooperate to shape the cell type-specific transcriptome. *Nature Communications* **2021**, *12*, 3885.
- (17) Prorok, P.; Artufel, M.; Aze, A.; Coulombe, P.; Peiffer, I.; Lacroix, L.; Guédin, A.; Mergny, J.-L.; Damaschke, J.; Schepers, A.; others Involvement of G-quadruplex regions in mammalian replication origin activity. *Nature Communications* **2019**, *10*, 3274.
- (18) Chen, X.; Yuan, J.; Xue, G.; Campanario, S.; Wang, D.; Wang, W.; Mou, X.; Liew, S. W.; Umar, M. I.; Isern, J.; others Translational control by DHX36 binding to 5' UTR G-quadruplex is essential for muscle stem-cell regenerative functions. *Nature Communications* **2021**, *12*, 5043.
- (19) Georgakopoulos-Soares, I.; Parada, G. E.; Wong, H. Y.; Medhi, R.; Furlan, G.; Munita, R.; Miska, E. A.; Kwok, C. K.; Hemberg, M. Alternative splicing modulation by G-quadruplexes. *Nature Communications* **2022**, *13*, 2404.
- (20) Biffi, G.; Tannahill, D.; McCafferty, J.; Balasubramanian, S. Quantitative visualization of DNA G-quadruplex structures in human cells. *Nature Chemistry* **2013**, *5*, 182–186.
- (21) Summers, P. A.; Lewis, B. W.; Gonzalez-Garcia, J.; Porreca, R. M.; Lim, A. H.; Cadinu, P.; Martin-Pintado, N.; Mann, D. J.; Edel, J. B.; Vannier, J. B.; others Visualising G-quadruplex DNA dynamics in live cells by fluorescence lifetime imaging microscopy. *Nature Communications* **2021**, *12*, 162.
- (22) Mulholland, K.; Wu, C. Binding of telomestatin to a telomeric G-quadruplex DNA probed by all-atom molecular dynamics simulations with explicit solvent. *Journal of chemical information and modeling* **2016**, *56*, 2093–2102.
- (23) Wu, W.-Q.; Zhang, M.-L.; Song, C.-P. A comprehensive evaluation of a typical plant

- telomeric G-quadruplex (G4) DNA reveals the dynamics of G4 formation, rearrangement, and unfolding. *Journal of Biological Chemistry* **2020**, *295*, 5461–5469.
- (24) Rider, S. D.; Gadgil, R. Y.; Hitch, D. C.; Damewood, F. J.; Zavada, N.; Shanahan, M.; Alhawach, V.; Shrestha, R.; Shin-Ya, K.; Leffak, M. Stable G-quadruplex DNA structures promote replication-dependent genome instability. *Journal of Biological Chemistry* **2022**, *298*.
- (25) Jiang, M.; Hu, H.; Zhao, K.; Di, R.; Huang, X.; Shi, Y.; Yue, Y.; Nie, J.; Yu, S.; Wang, W.; others The G4 resolvase RHAU modulates mRNA translation and stability to sustain postnatal heart function and regeneration. *Journal of Biological Chemistry* **2021**, *296*.
- (26) De Magis, A.; Götz, S.; Hajikazemi, M.; Fekete-Szücs, E.; Caterino, M.; Juranek, S.; Paeschke, K. Zuo1 supports G4 structure formation and directs repair toward nucleotide excision repair. *Nature Communications* **2020**, *11*, 3907.
- (27) Jain, A. K.; Paul, A.; Maji, B.; Muniyappa, K.; Bhattacharya, S. Dimeric 1, 3-phenylene-bis (piperazinyl benzimidazole) s: synthesis and structure–activity investigations on their binding with human telomeric G-quadruplex DNA and telomerase inhibition properties. *Journal of Medicinal Chemistry* **2012**, *55*, 2981–2993.
- (28) Liu, S.; Wang, Z.; Shah, S. B.; Chang, C.-Y.; Ai, M.; Nguyen, T.; Xiang, R.; Wu, X. DNA repair protein RAD52 is required for protecting G-quadruplexes in mammalian cells. *Journal of Biological Chemistry* **2023**, *299*.
- (29) Kosiol, N.; Juranek, S.; Brossart, P.; Heine, A.; Paeschke, K. G-quadruplexes: A promising target for cancer therapy. *Molecular Cancer* **2021**, *20*, 1–18.
- (30) Ali, A.; Bansal, M.; Bhattacharya, S. Ligand 5, 10, 15, 20-tetra (N-methyl-4-pyridyl) porphine (TMPyP4) prefers the parallel propeller-type human telomeric G-quadruplex DNA over its other polymorphs. *The Journal of Physical Chemistry B* **2015**, *119*, 5–14.

- (31) Calabrese, D. R.; Chen, X.; Leon, E. C.; Gaikwad, S. M.; Phyto, Z.; Hewitt, W. M.; Alden, S.; Hilimire, T. A.; He, F.; Michalowski, A. M.; others Chemical and structural studies provide a mechanistic basis for recognition of the MYC G-quadruplex. *Nature Communications* **2018**, *9*, 4229.
- (32) Paul, R.; Dutta, D.; Das, T.; Debnath, M.; Dash, J. G4 Sensing Pyridyl-Thiazole Polyamide Represses c-KIT Expression in Leukemia Cells. *Chemistry—A European Journal* **2021**, *27*, 8590–8599.
- (33) Pandya, N.; Singh, M.; Rani, R.; Kumar, V.; Kumar, A. G-quadruplex-mediated specific recognition, stabilization and transcriptional repression of bcl-2 by small molecule. *Archives of Biochemistry and Biophysics* **2023**, *734*, 109483.
- (34) Membrino, A.; Cogoi, S.; Pedersen, E. B.; Xodo, L. E. G4-DNA formation in the HRAS promoter and rational design of decoy oligonucleotides for cancer therapy. *PLOS One* **2011**, *6*, e24421.
- (35) Wang, K.-B.; Liu, Y.; Li, J.; Xiao, C.; Wang, Y.; Gu, W.; Li, Y.; Xia, Y.-Z.; Yan, T.; Yang, M.-H.; others Structural insight into the bulge-containing KRAS oncogene promoter G-quadruplex bound to berberine and coptisine. *Nature Communications* **2022**, *13*, 6016.
- (36) Zhu, B.-C.; He, J.; Liu, W.; Xia, X.-Y.; Liu, L.-Y.; Liang, B.-B.; Yao, H.-G.; Liu, B.; Ji, L.-N.; Mao, Z.-W. Selectivity and Targeting of G-Quadruplex Binders Activated by Adaptive Binding and Controlled by Chemical Kinetics. *Angewandte Chemie* **2021**, *133*, 15468–15471.
- (37) Wang, E.; Thombre, R.; Shah, Y.; Latanich, R.; Wang, J. G-Quadruplexes as pathogenic drivers in neurodegenerative disorders. *Nucleic Acids Research* **2021**, *49*, 4816–4830.

- (38) Machireddy, B.; Kalra, G.; Jonnalagadda, S.; Ramanujachary, K.; Wu, C. Probing the binding pathway of BRACO19 to a parallel-stranded human telomeric G-quadruplex using molecular dynamics binding simulation with AMBER DNA OL15 and ligand GAFF2 force fields. *Journal of chemical information and modeling* **2017**, *57*, 2846–2864.
- (39) Sullivan, H.-J.; Chen, B.; Wu, C. Molecular dynamics study on the binding of an anticancer DNA G-quadruplex stabilizer, CX-5461, to human telomeric, c-KIT1, and c-Myc G-quadruplexes and a DNA duplex. *Journal of chemical information and modeling* **2020**, *60*, 5203–5224.
- (40) Cui, Y.; Liu, H.; Ming, Y.; Zhang, Z.; Liu, L.; Liu, R. Prediction of strand-specific and cell-type-specific G-quadruplexes based on high-resolution CUT&Tag data. *Briefings in Functional Genomics* **2023**, elad024.
- (41) Huppert, J. L.; Balasubramanian, S. Prevalence of quadruplexes in the human genome. *Nucleic Acids Research* **2005**, *33*, 2908–2916.
- (42) Law, M. J.; Lower, K. M.; Voon, H. P.; Hughes, J. R.; Garrick, D.; Viprakasit, V.; Mitson, M.; De Gobbi, M.; Marra, M.; Morris, A.; others ATR-X syndrome protein targets tandem repeats and influences allele-specific expression in a size-dependent manner. *Cell* **2010**, *143*, 367–378.
- (43) Gray, L. T.; Vallur, A. C.; Eddy, J.; Maizels, N. G quadruplexes are genomewide targets of transcriptional helicases XPB and XPD. *Nature Chemical Biology* **2014**, *10*, 313–318.
- (44) Kumari, S.; Bugaut, A.; Huppert, J. L.; Balasubramanian, S. An RNA G-quadruplex in the 5' UTR of the NRAS proto-oncogene modulates translation. *Nature Chemical Biology* **2007**, *3*, 218–221.
- (45) Kudlicki, A. S. G-quadruplexes involving both strands of genomic DNA are highly

- abundant and colocalize with functional sites in the human genome. *PLoS One* **2016**, *11*, e0146174.
- (46) Varizhuk, A.; Ischenko, D.; Tsvetkov, V.; Novikov, R.; Kulemin, N.; Kaluzhny, D.; Vlasenok, M.; Naumov, V.; Smirnov, I.; Pozmogova, G. The expanding repertoire of G4 DNA structures. *Biochimie* **2017**, *135*, 54–62.
- (47) Varizhuk, A.; Ischenko, D.; Smirnov, I.; Tatarinova, O.; Severov, V.; Novikov, R.; Tsvetkov, V.; Naumov, V.; Kaluzhny, D.; Pozmogova, G. An improved search algorithm to find G-quadruplexes in genome sequences. *bioRxiv* **2014**, 001990.
- (48) Hon, J.; Martínek, T.; Zendulka, J.; Lexa, M. pqsfinder: an exhaustive and imperfection-tolerant search tool for potential quadruplex-forming sequences in R. *Bioinformatics* **2017**, *33*, 3373–3379.
- (49) Labudová, D.; Hon, J.; Lexa, M. pqsfinder web: G-quadruplex prediction using optimized pqsfinder algorithm. *Bioinformatics* **2020**, *36*, 2584–2586.
- (50) Bedrat, A.; Lacroix, L.; Mergny, J.-L. Re-evaluation of G-quadruplex propensity with G4Hunter. *Nucleic Acids Research* **2016**, *44*, 1746–1759.
- (51) Brázda, V.; Kolomazník, J.; Lýsek, J.; Bartas, M.; Fojta, M.; Št’astný, J.; Mergny, J.-L. G4Hunter web application: a web server for G-quadruplex prediction. *Bioinformatics* **2019**, *35*, 3493–3495.
- (52) Lacroix, L. G4HunterApps. *Bioinformatics* **2019**, *35*, 2311–2312.
- (53) Chambers, V. S.; Marsico, G.; Boutell, J. M.; Di Antonio, M.; Smith, G. P.; Balasubramanian, S. High-throughput sequencing of DNA G-quadruplex structures in the human genome. *Nature Biotechnology* **2015**, *33*, 877–881.
- (54) Hänsel-Hertsch, R.; Spiegel, J.; Marsico, G.; Tannahill, D.; Balasubramanian, S. Genome-wide mapping of endogenous G-quadruplex DNA structures by chromatin im-

- munoprecipitation and high-throughput sequencing. *Nature Protocols* **2018**, *13*, 551–564.
- (55) Sahakyan, A. B.; Chambers, V. S.; Marsico, G.; Santner, T.; Di Antonio, M.; Balasubramanian, S. Machine learning model for sequence-driven DNA G-quadruplex formation. *Scientific reports* **2017**, *7*, 14535.
- (56) Klimentova, E.; Polacek, J.; Simecek, P.; Alexiou, P. PENGUINN: Precise exploration of nuclear G-quadruplexes using interpretable neural networks. *Frontiers in Genetics* **2020**, *11*, 568546.
- (57) Barshai, M.; Aubert, A.; Orenstein, Y. G4detector: convolutional neural network to predict DNA G-quadruplexes. *IEEE/ACM Transactions on Computational Biology and Bioinformatics* **2021**, *19*, 1946–1955.
- (58) Rocher, V.; Genais, M.; Nassereddine, E.; Mourad, R. DeepG4: a deep learning approach to predict cell-type specific active G-quadruplex regions. *PLOS Computational Biology* **2021**, *17*, e1009308.
- (59) Korsakova, A.; Phan, A. T. Prediction of G4 formation in live cells with epigenetic data: a deep learning approach. *NAR Genomics and Bioinformatics* **2023**, *5*, lqad071.
- (60) He, K.; Zhang, X.; Ren, S.; Sun, J. Deep residual learning for image recognition. Proceedings of the IEEE conference on computer vision and pattern recognition. 2016; pp 770–778.
- (61) Mukherjee, S.; Ghosh, M.; Basuchowdhuri, P. DeepGLSTM: deep graph convolutional network and LSTM based approach for predicting drug-target binding affinity. Proceedings of the 2022 SIAM International Conference on Data Mining (SDM). 2022; pp 729–737.

- (62) Guedin, A.; Gros, J.; Alberti, P.; Mergny, J.-L. How long is too long? Effects of loop size on G-quadruplex stability. *Nucleic Acids Research* **2010**, *38*, 7858–7868.
- (63) Mukundan, V. T.; Phan, A. T. Bulges in G-quadruplexes: broadening the definition of G-quadruplex-forming sequences. *Journal of the American Chemical Society* **2013**, *135*, 5017–5028.
- (64) Maity, A.; Winnerdy, F. R.; Chang, W. D.; Chen, G.; Phan, A. T. Intra-locked G-quadruplex structures formed by irregular DNA G-rich motifs. *Nucleic Acids Research* **2020**, *48*, 3315–3327.
- (65) Jiang, M.; Anderson, J.; Gillespie, J.; Mayne, M. uShuffle: a useful tool for shuffling biological sequences while preserving the k-let counts. *BMC Bioinformatics* **2008**, *9*, 1–11.
- (66) Barshai, M.; Tripto, E.; Orenstein, Y. Identifying regulatory elements via deep learning. *Annual Review of Biomedical Data Science* **2020**, *3*, 315–338.
- (67) Bahdanau, D.; Cho, K.; Bengio, Y. Neural machine translation by jointly learning to align and translate. *arXiv preprint arXiv:1409.0473* **2014**,
- (68) Kingma, D. P.; Ba, J. Adam: A method for stochastic optimization. *arXiv preprint arXiv:1412.6980* **2014**,
- (69) Marsico, G.; Chambers, V. S.; Sahakyan, A. B.; McCauley, P.; Boutell, J. M.; Antonio, M. D.; Balasubramanian, S. Whole genome experimental maps of DNA G-quadruplexes in multiple species. *Nucleic Acids Research* **2019**, *47*, 3862–3874.